Vibroacoustic response of an immersed stiffened multilayered shell excited by a plane wave

M. Dana, L. Maxit, J. Bernard

inter.noise
HAMBURG 2016

Vibroacoustic response of an immersed stiffened multilayered shell excited by a plane wave

M. Dana[1,2], L. Maxit[1] and J. Bernard[2]
[1]Laboratory of Vibrations and Acoustics, INSA Lyon, France
[2]Thales Underwater Systems, Sofia Antipolis, France

ABSTRACT
The modelling of the vibroacoustic response of a periodically rib-stiffened cylindrical multilayered shell is of great interest in numerous industrial applications, among which submarine acoustics. An approach is proposed in this paper to couple an immersed multilayered shell model with models of the axisymmetric stiffeners. The multilayered shell may be modeled either with the transfer matrix method (TMM) or with the direct global method (DGM). Both methods are spectral: displacements and stress are obtained in the wavenumber domain before reconstructing the solution in the physical domain. This allows us representing different types of layers: isotropic, orthotropic, fluid, etc. The stiffeners are coupled to the multilayered shell at the internal radius of the latter. They are introduced in the formulation by dynamic circumferential admittances which are estimated by classic finite element methods. To illustrate the method we'll present different results as much for validation as for comparison with the unstiffened shell.

Keywords: Sound, Insulation, Transmission

1. INTRODUCTION

In military naval industry, designing submarines antennas can be of great complexity, especially the flank antennas for which to determine an accurate signal response is of crucial interest. A reliable configuration for modeling such a problem is to consider a cylindrical multilayered structure stiffened at its inner radius by a periodic network of stiffeners, and excited by an incident plane wave at its outer radius. The goal of this article is to develop an analytical method for the coupling of the stiffeners to the multilayered structure for reconstructing the pressure field at the antenna radius. Many spectral methods already cover the problem of modeling the same unribbed structure excited by a plane wave [1–5], and always remain on the same principle: first one has to solve the problem in each layer of the structure, then to find a way of assembly the whole system in order to represent the multilayered structure behaviour. Two of them retained our attention in this article: one is the direct global method, inspired from [1, 2] and limited to isotropic solid layers or fluid layers and use a Helmholtz decomposition then assembles the system with a global matrix; the other is the transfer matrix method, inspired from [3–5] and establishes a relation between the strain-displacement state vector at both ends of an elementary layer. This enables to propagate the vector state from an end to an other of the multilayered structure, the method is adapted to handle both orthotropic or isotropic layers, but suffers instability when introducing intermediate fluid layers. Therefore, the formalism retained for the coupling with the stiffeners shall adapt to either modeling method retained for describing the unribbed problem. We present briefly in Sec. 2 the full problem to be solved, then we introduce in Sec. 3 the developed formalism on how to couple the stiffeners to the unribbed shell. We highlight quantities one should compute to achieve the calculation of the pressure field at the sensor radius when the shell is coupled to the stiffeners. Then we detail in Sec. 4 the way of getting these quantities for each of both methods retained for the modeling of the unribbed multilayered shell. Finally we'll present results for each method in Sec. 5.

2. PRESENTATION OF THE PROBLEM

We consider a multilayered cylindrical structure ribbed by a network of equally spaced stiffeners of a distance d, as represented on Fig. 1:

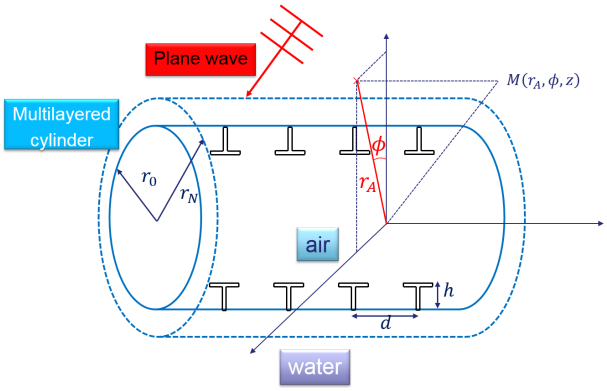

Figure 1: Multilayered cylindrical shell

It is supposed axisymmetric and of infinite length along its axis, which justifies the Fourier transform (1) used for switching from either the physical domain or the spectral domain:

$$\begin{aligned} F(r,\phi,z) &= \frac{1}{2\pi}\sum_{-\infty}^{+\infty} e^{in\phi}\int_{-\infty}^{+\infty}\tilde{F}(r,n,\alpha)e^{i\alpha z}d\alpha \\ \tilde{F}(r,n,\alpha) &= \frac{1}{2\pi}\int_0^{2\pi} e^{-in\phi}\int_{-\infty}^{+\infty}F(r,\phi,z)e^{-i\alpha z}dzd\phi \end{aligned} \tag{1}$$

The various layers are numbered from 1 being the steel shell to N being the last coating, and with 0 and $N+1$ being respectively the air filling the internal cavity and the water occupying the semi-infinite exterior domain.

The stiffeners are connected at the inner radius of the structure, equally spaced along its axis with a distance d.

The sensor is supposed to be punctual and placed into the external fluid, at a radius r_A. The multilayered structure is therefore subject to several excitations: the fluid loadings, the stress applied by the stiffeners network at the inner radius r_0, and the plane wave exciting its outer radius r_N. In these conditions, assuming the polar angle of the incident unit plane wave to be ϕ_i, α_0^i its wavenumber and c_e the compression waves velocity in the external fluid, the pressure field is known to be of the form:

$$p_T(r,n,\alpha) = p_b(r,n,\alpha) + p_e(r,n,\alpha) \tag{2}$$

$$\begin{cases} p_b(r,n,\alpha) = 2\pi(-i)^n e^{-in\phi_i}\left[J_n(\gamma_{|\alpha_0^i}r) - \dfrac{J_n'(\gamma_{|\alpha_0^i}r_N)}{H_n'(\gamma_{|\alpha_0^i}r_N)}H_n(\gamma_{|\alpha_0^i}r)\right]\delta_{|\alpha_0^i}(\alpha) \\ p_e(r,n,\alpha) = Z_{fle}(r,n)u_N(r_N,n,\alpha)\cdot\boldsymbol{e_r} \end{cases}$$

with $\delta_{|\alpha_0^i}(\alpha) = \delta(\alpha-\alpha_0^i)$ being the Dirac function shifted around the incident wavenumber α_0^i.

The external fluid impedance is $Z_{fle}(r,n) = \dfrac{\rho_e\omega^2 H_n(\gamma(\alpha_0^i)r)}{\gamma(\alpha_0^i)H_n'(\gamma(\alpha_0^i)r_N)}$ with $\gamma(\alpha) = \sqrt{k^2-\alpha^2}$ and $k = \dfrac{\omega}{c_e}$.

It is then necessary to determine the displacements field at the outer radius to reconstruct the pressure field at the sensor radius. Concerning the stress field at the outer radius, one can deduce from (2):

$$\begin{aligned} &\sigma_N(r_N,n,\alpha) = \sigma_{N,\mathrm{PW}}(r_N,n,\alpha) + \sigma_{fle}(r_N,n,\alpha) \\ &\text{with: } \begin{cases} \sigma_{N,\mathrm{PW}}(r_N,n,\alpha) = -p_b(r_N,n,\alpha)\boldsymbol{e_r} \\ \sigma_{fle}(r_N,n,\alpha) = -p_e(r_N,n,\alpha)\boldsymbol{e_r} \end{cases} \end{aligned} \tag{3}$$

At the inner radius we have:

$$\sigma_1(r_0,n,\alpha) = \sigma_{fli}(r_0,n,\alpha) + \sigma_{1r}(r_0,n,\alpha) \tag{4}$$

The stress field due to the internal fluid loading is
$\sigma_{fli}(r_0, n, \alpha) = p_{1i}(r_0, n, \alpha)\boldsymbol{e_r} = Z_{fli}(r_0, n, \alpha)\,(u_1(r_0, n, \alpha) \cdot \boldsymbol{e_r})\,\boldsymbol{e_r}$.
The internal fluid impedance is $Z_{fli}(r, n, \alpha) = \dfrac{\rho_i \omega^2 J_n(\gamma_i(\alpha) r)}{\gamma_i(\alpha) J_n'(\gamma_i(\alpha) r_0)}$ with $\gamma_i(\alpha) = \sqrt{k_i^2 - \alpha^2}$ and $k_i = \dfrac{\omega}{c_i}$
The stress field σ_{1r} is due to the periodic stiffeners network.

3. CALCULUS METHOD OF THE STRESS AND DISPLACEMENTS AT THE INNER RADIUS

We detail in this section a way of computing the displacements $u_1(r_0, n, \alpha)$ at the inner radius when the multilayered shell is coupled to the stiffeners and is excited by the plane wave. The pressure at the sensor position will be deduced from these displacements in a last step of the calculation.

3.1 Superposition principle

To determine the displacements induced at the inner radius $u_1(r_0, n, \alpha)$, the linearity of the system allows to break down fhe full problem of the multilayered structure into two sub-problems, as shown in Fig. 2:

- the unribbed free shell excited by the plane wave at its outer radius (see Fig. 2(b))
  The displacements field generated at the inner radius is noted $u_{1,\text{PW}}(r_0, n, \alpha)$.
- the stiffened shell at its inner radius when no other excitation applies other than the fluid loadings (see Fig. 2(c)).
  The displacements field generated at the inner radius by the periodic stiffeners network is noted $u_{1r}(r_0, n, \alpha)$.

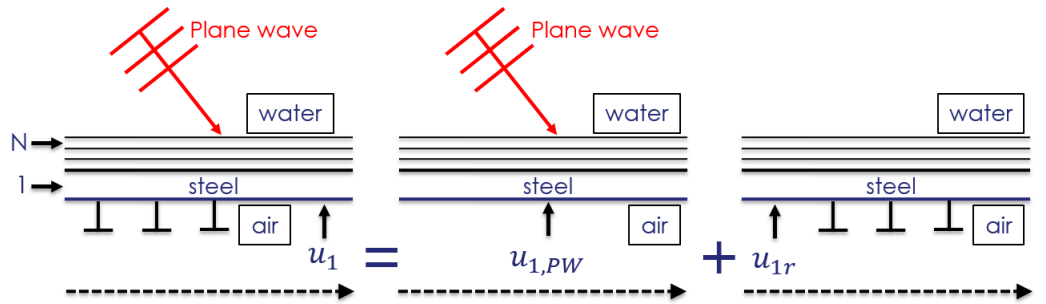

(a) Full problem (b) Plane wave excitation (c) stiffeners network excitation

Figure 2: Superposition principle

One can then write the following equation:

$$u_1(r_0, n, \alpha) = u_{1,\text{PW}}(r_0, n, \alpha) + u_{1r}(r_0, n, \alpha) \tag{5}$$

3.2 Admittance matrix and equivalent plane wave stress at the inner radius

In this approach, one need to compute two specific quantities in order to finalize the calculation.
First, for connecting the displacements and stress fields at the air-steel interface, one must introduce the admittance matrix $R(n, \alpha)$ of the fluid-loaded multilayered shell defined at the inner radius as follows:

$$u_1(r_0, n, \alpha) = R(n, \alpha)\sigma_1^\star(r_0, n, \alpha) \tag{6}$$

where $\sigma_1^\star(r_0, n, \alpha)$ is the stress field generated by the different external constraints applied at the inner radius other than the internal fluid loading. One can underline that the admittance matrix takes into account both external and internal fluid loads.

Knowing this admittance matrix $R(n,\alpha)$, one can immediately get the displacement of the shell at the inner radius due to the stiffeners stress field:

$$u_{1r}(r_0,n,\alpha) = R(n,\alpha)\sigma_{1r}(r_0,n,\alpha) \tag{7}$$

From the displacement field generated at the inner radius by the plane wave excitation at the outer radius in the sub-problem 2(b), one can deduce the equivalent plane wave stress field $\sigma_{1,\text{PWeq}}(r_0,n,\alpha)$ at the inner radius such that:

$$\sigma_{1,\text{PWeq}}(r_0,n,\alpha) = R^{-1}(n,\alpha)u_{1,\text{PW}}(r_0,n,\alpha) \tag{8}$$

Therefore, using Eq. (6) and (7), Eq. (5) can be rewritten:

$$u_1(r_0,n,\alpha) = R(n,\alpha)\left[\sigma_{1,\text{PWeq}}(r_0,n,\alpha) + \sigma_{1r}(r_0,n,\alpha)\right] \tag{9}$$

At this stage of the calculation the stiffeners network contribution to the stress field remains to be determined, which is the subject of the following part 3.3.
Then we'll explain on how to get the admittance matrix and the equivalent plane wave stress for each modeling method of the multilayered structure in 4.

3.3 Calculus of the stiffeners contribution

3.3.1 Finite element modeling of the stiffeners

The choice was made to model the axisymetrical stiffeners of the network by shell elements, which entails the taking into account of 4 degrees of freedom at each node of the mesh represented in Fig. 3 :

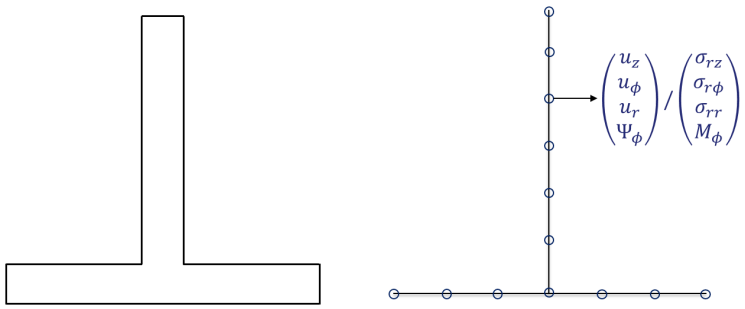

(a) Rib geometry (b) Shell elements modeling

Figure 3: Modeling of any stiffener

The fourth degree of freedom introduced is the rotation angle around the circonferential axis, which verifies the relationship:

$$\Psi_\phi(r,\phi,z) = \frac{\partial u_r}{\partial z}(r,\phi,z) \tag{10}$$

Besides, the meridional moment per surface unit M_ϕ introduced by the rotation angle is assumed to verify:

$$M_\phi(r,\phi,z) = \frac{\partial \sigma_{rr}}{\partial z}(r,\phi,z) \tag{11}$$

Furthermore, one can define for any stiffener the dynamic stiffness matrix $[B(n)]$ which connects these degrees of freedom and the forces this stiffener suffers at the nodes in contact with the steel shell at the inner radius, which are the cylinder attachments points $(r_0, z = qd)$.
By applying the principle of reciprocal actions, one can establish a relationship between the displacements at the air-steel interface and the stress undergone by the steel shell at the inner radius:

$$[B(n)]\begin{pmatrix} u_{z1} \\ u_{\phi 1} \\ u_{r1} \\ \Psi_1 \end{pmatrix}(r_0,n,z=qd) = -\begin{pmatrix} \sigma_{1rz} \\ \sigma_{1r\phi} \\ \sigma_{1rr} \\ M_{1\phi} \end{pmatrix}(r_0,n,z=qd) \tag{12}$$

One can observe from Equation (12) that displacements and stress at the inner radius shall be extended to take into account the angle of rotation and its induced meridional moment:

$$\begin{aligned} u_1 &= (u_{z1}, u_{\phi 1}, u_{r1})^T \quad \rightarrow \overline{u}_1 = (u_{z1}, u_{\phi 1}, u_{r1}, \Psi_1)^T \\ \sigma_{1r} &= (\sigma_{1rz}, \sigma_{1r\phi}, \sigma_{1rr})^T \rightarrow \overline{\sigma}_{1r} = (\sigma_{1rz}, \sigma_{1r\phi}, \sigma_{1rr}, M_{1\phi})^T \\ \sigma_{1,\text{PWeq}} &= (0, 0, \sigma_{1,\text{PWeq}} \cdot \boldsymbol{e_r})^T \rightarrow \overline{\sigma}_{1,\text{PWeq}} = (0, 0, \sigma_{1,\text{PWeq}} \cdot \boldsymbol{e_r}, 0)^T \end{aligned} \tag{13}$$

Therefore, extending the theoretical stress field $\sigma_1^\star$ involved in (6) into $\overline{\sigma_1^\star} = \overline{\sigma}_{1,\text{PWeq}} + \overline{\sigma}_{1r}$ and using (10)-(11) enables to extend as well the admittance matrix defined before:

$$\begin{pmatrix} R_{11} & R_{12} & R_{13} & R_{14} \\ R_{21} & R_{22} & R_{23} & R_{24} \\ R_{31} & R_{32} & R_{33} & R_{34} \\ R_{41} & R_{42} & R_{43} & R_{44} \end{pmatrix} \overline{\sigma}_{1r}(r_0, n, \alpha) = \overline{u}_{1r}(r_0, n, \alpha) \tag{14}$$

$$\text{avec: } \begin{cases} R_{14}(n,\alpha) = -i\alpha R_{13}(n,\alpha), \quad R_{41}(n,\alpha) = i\alpha R_{31}(n,\alpha) \\ R_{24}(n,\alpha) = -i\alpha R_{23}(n,\alpha), \quad R_{42}(n,\alpha) = i\alpha R_{32}(n,\alpha) \\ R_{34}(n,\alpha) = -i\alpha R_{33}(n,\alpha), \quad R_{43}(n,\alpha) = i\alpha R_{33}(n,\alpha) \\ R_{44}(n,\alpha) = \alpha^2 R_{33}(n,\alpha) \end{cases}$$

From now on, the extension to the rotation angle is considered to be done at the inner radius for the displacements and stress fields, as well as for the admittance matrix, and we omit the bar symbol over the fields letters.

3.3.2 Stress field applied by the stiffeners network

Once this extent has been done, one can define the stress field applied by the periodic stiffeners network using (12):

$$\begin{aligned} \sigma_{1r}(r_0, n, z) &= \sum_{q=-\infty}^{\infty} \sigma_{1r}(r_0, n, z = qd)\delta(z - qd) \\ &= -\left[B(n)\right] \sum_{q=-\infty}^{\infty} u_1(r_0, n, z = qd)\delta(z - qd) \end{aligned} \tag{15}$$

One can therefore establish the expression for the stress applied by the stiffeners network in the spectral domain, after applying a Poisson relation:

$$\sigma_{1r}(r_0, n, \alpha) = -\frac{1}{d}\left[B(n)\right] \sum_{q=-\infty}^{\infty} u_1\left(r_0, n, \alpha + \frac{2\pi q}{d}\right) \tag{16}$$

Using (9) and (16) leads to:

$$u_1(r_0, n, \alpha) = R(n,\alpha)\sigma_{1,\text{PWeq}}(r_0, n, \alpha) - \frac{1}{d}R(n,\alpha)\left[B(n)\right] \sum_{q=-\infty}^{\infty} u_1\left(r_0, n, \alpha + \frac{2\pi q}{d}\right) \tag{17}$$

Therefore it is possible to determine the sum of the displacements $\sum_{q=-\infty}^{\infty} u_1\left(r_0, n, \alpha + \frac{2\pi q}{d}\right)$ and establish an explicit expression for the periodic stiffeners network contribution of stress:

$$\begin{aligned} \sigma_{1r}(r_0, n, \alpha) = -\frac{1}{d}\left[B(n)\right] \Bigg[\text{Id} + \frac{1}{d}\Bigg\{ \sum_{q=-\infty}^{\infty} R\left(n, \alpha + \frac{2\pi q}{d}\right) \Bigg\} \left[B(n)\right]\Bigg]^{-1} \times \\ \sum_{q=-\infty}^{\infty} R(n,\alpha)\sigma_{1,\text{PWeq}}\left(r_0, n, \alpha + \frac{2\pi q}{d}\right) \end{aligned} \tag{18}$$

Finally, the displacement field at the inner radius is given by introducing (18) in (9).

4. SPECTRAL METHODS FOR MODELING THE MULTILAYERED STRUCTURE RESPONSE APPLIED TO THE COUPLING

We detail in this section how to adapt two spectral methods to the established formalism for coupling the multilayered structure to the periodic stiffeners network. In each method we shall present the main principle, how to get the admittance matrix and the equivalent plane wave at the inner radius, and finally how to reconstruct the pressure field at the sensor radius.

4.1 Direct global method

4.1.1 Principle of the DGM

The direct global method relies on a Helmholtz decomposition of the displacements and stress fields inside each elementary layer of the multilayered structure. The elementary matrices connecting the displacements and stress to the coefficients of the Helmholtz decomposition are constructed under the assumption that:

- for a fluid layer, the acoustic pressure is solution of the Helmholtz equation
- for a solid layer, the displacements field is decomposed in a sum of scalar and vector potentials solutions of the Helmholtz equation [1, 2].

Therefore, if we note $\boldsymbol{F}$ and $\boldsymbol{B}$ respectively a fluid and solid matrix of an arbitrary layer we can write:

$$\begin{aligned}
&\text{•Fluid layer:} \quad \begin{pmatrix} u_r(r,n,\alpha) \\ \sigma_{rr}(r,n,\alpha) \end{pmatrix} = \boldsymbol{F}(r,n,\alpha) \begin{pmatrix} A_1 \\ A_2 \end{pmatrix}(n,\alpha) \\
&\text{•Solid layer:} \quad \begin{pmatrix} u_r(r,n,\alpha) \\ u_\phi(r,n,\alpha) \\ u_z(r,n,\alpha) \\ \sigma_{rr}(r,n,\alpha) \\ \sigma_{r\phi}(r,n,\alpha) \\ \sigma_{rz}(r,n,\alpha) \end{pmatrix} = \boldsymbol{B}(r,n,\alpha) \begin{pmatrix} A_1 \\ A_2 \\ A_3 \\ A_4 \\ A_5 \\ A_6 \end{pmatrix}(n,\alpha)
\end{aligned} \tag{19}$$

The coefficients of the elementary matrices can be found in [1], then we use it to express the conditions of continuity between layers and to assembly the global matrix involved in the system below describing the multilayered structure:

$$Z(n,\alpha)\{X\}(n,\alpha) = E(n,\alpha) \tag{20}$$

where $Z(n,\alpha)$ is the global matrix of the system, invariant from the excitation chosen, which is characterized by the excitation vector $E(n,\alpha)$. $\{X\}(n,\alpha)$ contains the elementary coefficients of each layer, and follows the shape:

$$\{X\}(n,\alpha) = \left(A_1^0 \quad A_2^0 \middle| A_1^1 \cdots A_6^1 \middle| \cdots \middle| A_1^N \cdots A_6^N \middle| A_1^{N+1} \quad A_2^{N+1} \right)^T (n,\alpha) \tag{21}$$

More details on the global matrix method can be found in [7].

4.1.2 Obtaining the admittance matrix and the equivalent plane wave stress

The direct global method allows to reconstruct the displacements field in the steel shell at the inner radius using the steel solid matrix evaluated at the same radius:

$$\boldsymbol{u}_1(r_0,n,\alpha) = B^1_{|r_0}(1:3,:)\{X\}(3:8,:) \tag{22}$$

Besides let consider the following point mechanical excitation σ_m applied at the point $(r_0, \phi_0 = 0, z_0 = 0)$ and written below in both physical and spectral domain:

$$\begin{aligned}
\sigma_m(r_0,\phi,z) &= 2\pi\delta(\phi)\delta(z)\cdot\boldsymbol{v} \\
\sigma_m(r_0,n,\alpha) &= 1\cdot\boldsymbol{v}
\end{aligned} \tag{23}$$

where $\boldsymbol{v}$ can be any of the three vectors of the cylindrical base $\boldsymbol{e_z}$, $\boldsymbol{e_\phi}$ ou $\boldsymbol{e_r}$.

Then let write the three displacement fields associated with each of the three different excitations represented in (23):

$$\begin{aligned}
&(\boldsymbol{v} = \boldsymbol{e_z} \iff \sigma_{rz} \text{ imposed}) \rightsquigarrow \boldsymbol{u}_{1|\sigma_{rz}} \\
&(\boldsymbol{v} = \boldsymbol{e_\phi} \iff \sigma_{r\phi} \text{ imposed}) \rightsquigarrow \boldsymbol{u}_{1|\sigma_{r\phi}} \\
&(\boldsymbol{v} = \boldsymbol{e_r} \iff \sigma_{rr} \text{ imposed}) \rightsquigarrow \boldsymbol{u}_{1|\sigma_{rr}}
\end{aligned} \tag{24}$$

Finally one can notice that each column of the admittance matrix $R(n,\alpha)$ is identical to the previous displacement fields:

$$\begin{aligned}
R(n,\alpha)\cdot\boldsymbol{e_z} &= \begin{pmatrix} R_{11}(n,\alpha) \\ R_{21}(n,\alpha) \\ R_{31}(n,\alpha) \end{pmatrix} = \boldsymbol{u}_{1|\sigma_{rz}} \\
R(n,\alpha)\cdot\boldsymbol{e_\phi} &= \begin{pmatrix} R_{12}(n,\alpha) \\ R_{22}(n,\alpha) \\ R_{32}(n,\alpha) \end{pmatrix} = \boldsymbol{u}_{1|\sigma_{r\phi}} \\
R(n,\alpha)\cdot\boldsymbol{e_r} &= \begin{pmatrix} R_{13}(n,\alpha) \\ R_{23}(n,\alpha) \\ R_{33}(n,\alpha) \end{pmatrix} = \boldsymbol{u}_{1|\sigma_{rr}}
\end{aligned} \tag{25}$$

The admittance matrix is then constructed by computing three different DGM calculations, where only the excitation vector changes. The final step is to get the displacements fields necessary to the construction of the admittance matrix:

$$R(n,\alpha) = \left(\boldsymbol{u}_{1|\sigma_{rz}} \middle| \boldsymbol{u}_{1|\sigma_{r\phi}} \middle| \boldsymbol{u}_{1|\sigma_{rr}} \right) \tag{26}$$

Once the admittance matrix is defined, one can also get the equivalent plane wave stress by computing an other DGM calculation, this time with the set of boundary conditions corresponding to the excitation by a plane wave of the unribbed multilayered structure at its outer radius r_N. Indeed, the displacements field in the steel shell at the inner radius r_0 that one can reconstruct from this calculation is identical to the product of the admittance matrix by the equivalent plane wave stress, so we have:

$$\sigma_{1,\text{PWeq}}(r_0,n,\alpha) = R^{-1}(n,\alpha)u_{1,\text{PW}}(r_0,n,\alpha) \tag{27}$$

4.1.3 Pressure field at the sensor radius

To reconstruct the pressure field at the sensor radius, we first get the stiffeners contribution $\sigma_{1r}(r_0,n,\alpha)$ to the stress field from equations (18), after calculating the admittance matrix and the equivalent plane wave as described above. Then a last DGM calculation is necessary to determine the displacements field in the last coating at the outer radius $u_{N,\text{ribs,OP}}(r_N,n,\alpha)$, computed with the set of boundary conditions of the full problem. To achieve this, the stress field $\sigma_{1r}(r_0,n,\alpha)$ already determined is used to complete the set of boundary conditions of the problem.

4.2 Transfer matrix method

4.2.1 Principle of the transfer matrix method

The transfer matrix method was more widely detailed in [7], here we only present the relation that one can get between the state vector containing the displacements and stress evaluated at both ends of the multilayered structure:

$$\begin{gathered}
\begin{pmatrix} u_N \\ \sigma_N \end{pmatrix}(r_N,n,\alpha) = \begin{pmatrix} T_{u_N u_1} & T_{u_N \sigma_1} \\ T_{\sigma_N u_1} & T_{\sigma_N \sigma_1} \end{pmatrix}(n,\alpha) \begin{pmatrix} u_1 \\ \sigma_1 \end{pmatrix}(r_0,n,\alpha) \\
\text{avec: } u = \left(u_z \; u_\phi \; u_{1r}\right)^T \text{ et } \sigma = \left(\sigma_{rz} \; \sigma_{r\phi} \; \sigma_{rr}\right)^T
\end{gathered} \tag{28}$$

The submatrices in the system (28) constitute the transfer matrix of the whole structure, which is found by multiplying the different transfer matrices of the elementary layers. The developments for getting the global transfer matrix can be found in [7].

4.2.2 *Obtaining the admittance matrix and the equivalent plane wave stress*

By using equations (4) and (3), one can get the following relationship between displacements and stress in the steel shell at the inner radius:

$$u_1(r_0,n,\alpha) = R(n,\alpha)\left[\sigma^0_{1,\text{PWeq}}(r_0,n,\alpha)\delta(\alpha-\alpha_0^i) + \sigma_{1r}(r_0,n,\alpha)\right] \tag{29}$$

with:

$$\begin{cases} R(n,\alpha) = (X^{-1}Y)(n,\alpha) \\ \sigma_{1,\text{PWeq}}(r_0,n,\alpha) = Y^{-1}(n,\alpha)\sigma_{N,\text{PW}}(r_N,n,\alpha) \\ X(n,\alpha) = -\left[T_{fle}T_{u_N u_1} + T_{\sigma_N u_1} + \left(T_{\sigma_N\sigma_1} + T_{fle}T_{u_N\sigma_1}\right)T_{fli}\right](n,\alpha) \\ Y(n,\alpha) = \left[T_{\sigma_N\sigma_1} + T_{fle}T_{u_N\sigma_1}\right](n,\alpha) \end{cases} \tag{30}$$

and T_{fli} and T_{fle} being defined as:

$$\begin{cases} T_{fli}(r,n,\alpha) = Z_{fli}(r,n,\alpha)\boldsymbol{e_r}\otimes\boldsymbol{e_r} \\ T_{fle}(r,n) = Z_{fle}(r,n)\boldsymbol{e_r}\otimes\boldsymbol{e_r} \end{cases} \tag{31}$$

4.2.3 *Pressure field at the sensor radius*

Finally, one can reconstruct the displacement field in the last coating at the outer radius $u_{N,\text{ribs,OP}}(r_N,n,\alpha)$ by using the first relation of the matrix system (28):

$$u_N(r_N,n,\alpha) = T_{u_N u_1}(n,\alpha)u_1(r_0,n,\alpha) + T_{u_N\sigma_1}(n,\alpha)\sigma_1(r_0,n,\alpha) \tag{32}$$

The pressure field can then be obtained with the relation (2).

5. RESULTS FOR BOTH METHODS ON A REDUCED RIBBED SHELL CONFIGURATION

In this section we finally present first validation results for the coupling formalism developed in Sec. 2-3 specific to the transfer matrix method concerning the modeling of the multilayered shell.

5.1 Numerical setup

The configuration used for the numerical computations is the same as in [8], concerning the shell and ribs dimensions, which is summarized in Table 1. The stiffeners are assumed to be of classic T-shape, and their section is rectangular. The last row of the following table reminds that the infinite series involved in Eq. 18 are truncated numerically into finite sums covering the range $[\![-Q;Q]\!]$.

Properties	Air	Steel	Water	Stiffener
Density (kg.m^{-3})	1.2 (ρ_i)	7900 (ρ_s)	1000 (ρ_e)	
Sound velocity (m.s^{-1})	340 (c_i)		1470 (c_e)	
Longitudinal velocity (m.s^{-1})		5790 (c_L)		
Transversal velocity (m.s^{-1})		3100 (c_T)		
Inner radius (cm)		0.49		
Outer radius (cm)		0.5		
Stiffeners network period (cm)				1.5 (d)
Height (cm)				0.5 (h)
Width (mm)				0.5 (h)
Number of stiffeners Q				10

Table 1: Numerical setup

The antenna is assumed to be only one ponctual sensor, its radius is worth $r_A = 6.04$ cm, and the axial position z_A along the shell axis can vary.

5.2 Results for the normal incidence

5.2.1 First validation on the pressure field

First we present in Fig. 4 the signal response according to the frequency of the multilayered shell when excited by a plane wave under normal incidence, for a sensor placed at different axial positions $z_A = 0$, $z_A = \frac{d}{2}$ and $z_A = d$.

The results are confronted to an already validated model which utilizes a thin shell assumption for describing the multilayered structure.

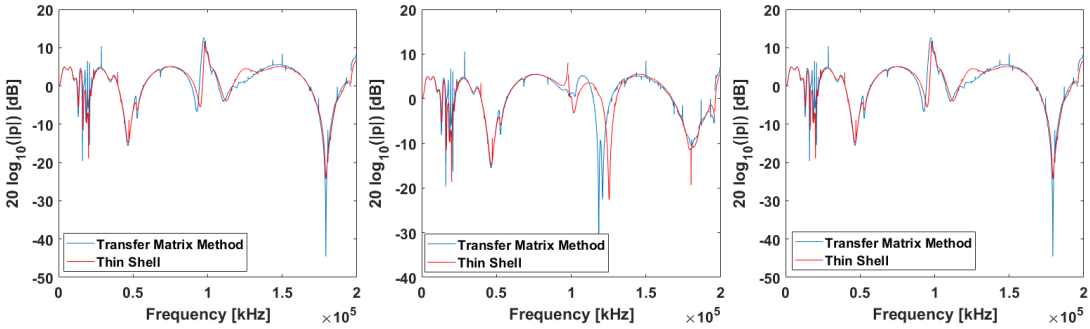

(a) $z_A = 0$ (b) $z_A = \frac{d}{2}$ (c) $z_A = d$

Figure 4: Signal response at the sensor radius for different axial positions

One can underline that the correlation of the two responses fade away with the increasing frequency, because the thin shell model is valid only at low frequency.
Both responses 4(a) and 4(b) are identical, because in these cases the sensor is placed at a coupling point of two consecutive stiffeners. This verdict enables to validate the periodicity of the system.

5.2.2 Second validation on the displacement field

Secondly, we present an analysis of the displacement field at the inner radius when the stiffener is supposed infinitly rigid about the radial dimension, in that configuration the shell is assumed simply supported at the coupling points with the stiffeners. In that case the dynamic stiffness $[B(n)]$ takes the following form:

$$[B(n)] = \begin{pmatrix} 0 & 0 & 0 & 0 \\ 0 & 0 & 0 & 0 \\ 0 & 0 & b_{33} & 0 \\ 0 & 0 & 0 & 0 \end{pmatrix}, b_{33} \to +\infty \tag{33}$$

This also entails perfect cancellation of the displacements at the different coupling points $z = qd$, therefore one can highlight this result by plotting the spatial displacements of the multilayered shell for a given frequency at the inner radius, as it is done in Fig. 5 for the normal displacement on the interval $z_A \in [\![-d, d]\!]$ at the frequency $f = 20$ kHz:

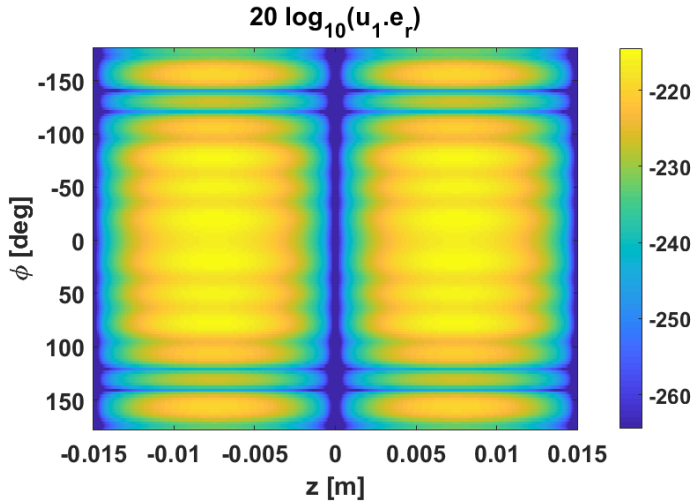

Figure 5: Displacements at the inner radius. $f = 20$ kHz, $z_A \in [\![-d, d]\!]$

One can see at the coupling points $z_A = 0, \pm d$ the cancellation of the displacement field at the inner radius.

6. CONCLUSION

In this article, we developed a formalism to model cylindrical multilayered ribbed shells. The developed formalism is adaptable to both direct global method or transfer matrix method which shall be retained for modeling the multilayered structure. The preliminary validation exposed in this article shall be followed with much deeper investigation, in particular a cross validation between the direct global method and the transfer matrix method, as well as a comparison between these last two with a finite element method.

REFERENCES

[1] E.A. Skelton, J.H. James, Theoretical acoustics of underwater structures, *Imperial College Press* (1997).

[2] D.C. Ricks, H. Schmidt, A numerically stable global matrix method for cylindrically layered shells excited by ring forces, *J. Acoust. Soc. Am.*, **95** (6), 3339-3349 (1994).

[3] J.R. Fan, Exact theory of strongly thick laminated plates and shells, *Beijing: Science Press* (1996).

[4] W.Q. Chen, Z.G. Bian, H.J. Ding, Three-dimensional vibration analysis of fluid-filled orthotropic FGM cylindrical shells, *International Journal of Mechanical Sciences* **46**, 159-171 (2004).

[5] C. Dutrion, *Étude de faisabilité d'un revêtement élastique pour la furtivité acoustique*, thèse de doctorat-ISAE (2014).

[6] M. Dana, Modélisation numérique de structures cylindriques multicouches excitées par une onde plane: comparaison de différentes méthodes, 5 ème édition des Journées Acoustique et Applications Navales (JAAN2017), Ollioules, 26-27 octobre 2017.

[7] M. Dana, L. Maxit, J. Bernard - Prédiction de la réponse vibro-acoustique de coques cylindriques revêtues immergées, 14 ème Congrès Français d'Acoustique (CFA2018), Le Havre, 23-27 avril 2018.

[8] R. Liétard, D. Décultot and G. Maze, Acoustic scattering from a finite cylindrical shell with evenly spaced stiffeners: Experimental investigation, *J. Acoust. Soc. Am.*, **118**, 2142-2146 (2005).

[9] A. J. Hull, J. R. Welch, Elastic response of an acoustic coating on a rib-stiffened plate, *Journal of Sound and Vibration*, **329**, 4192-4211 (2010).